

# Orientation Constraints in Point-Based Elastic Image Registration

Mike Fornefett, Karl Rohr, Rainer Sprengel\*, and H. Siegfried Stiehl

Universität Hamburg, Fachbereich Informatik,  
Arbeitsbereich Kognitive Systeme  
Vogt-Kölln-Str. 30, D-22527 Hamburg, Germany  
fornefett@informatik.uni-hamburg.de

**Abstract.** We present a new approach to incorporate orientation attributes at landmarks in an elastic medical image registration scheme. The approach is based on a minimizing functional and can cope with images of arbitrary dimensions. Constraints due to orientations are incorporated through scalar products between the transformed orientation vectors in the source image and vectors which are perpendicular to the orientation vectors in the target image. For synthetic data sets we show that the structure of rigid objects in an otherwise elastically deformed image can be preserved. The application of our approach to tomographic data sets shows that improvements w.r.t. accuracy can be achieved provided a sufficient number of landmarks is well-distributed over the image.

## 1 Introduction

Landmark-based elastic registration relies on the information associated with landmark points. To improve the results of landmark-based approaches while maintaining their efficiency, work in the past has been done on including additional landmark attributes, like orientation. Especially in medical applications it is desirable to improve the registration result without adding further landmarks.

Bookstein and Green [1] incorporate orientations by approximating them through two landmarks. Mardia et al. [3] use a kriging method to include derivative information. Their interpolation scheme yields an exact solution, but orientation vectors are required to be unit vectors. In this paper, we describe a new approach which i) is based on a minimizing functional and ii) allows to incorporate orientation attributes. As in the approach of Mardia et al. [3], exact orientations at landmarks are incorporated. However, in our case the directional constraints are represented through scalar products and therefore the lengths of the orientation vectors need not to be normalized to unit vectors. Another advantage of our approach is that it covers the full range from interpolation to approximation using a regularization parameter  $\lambda$ . In Sect. 2, we give an overview of our approach for the general case of  $d$ -dimensional images and in Sect. 3, we demonstrate the applicability of our approach for 2D and 3D images.

---

\* Now with debis Systemhaus GEI, Hamburg.

## 2 Approach

The inclusion of orientations at landmarks of two corresponding images means to constrain the transformation in the neighborhood of the landmarks in direction of the mapped orientations. Note, that it is possible to apply several constraining orientations at single landmarks. In our scheme the searched transformation function  $\mathbf{u} : \mathbb{R}^d \rightarrow \mathbb{R}^d$ , where  $d$  is the image dimension, minimizes the following functional:

$$\frac{1}{n} \sum_{i=1}^n (\mathbf{v}_i - L_i \mathbf{u})^2 + \lambda J_m^d(\mathbf{u}), \quad (1)$$

which can also be written as:

$$\frac{1}{dn+(d-1)n_\theta} \left( \sum_{i=1}^n (\mathbf{q}_i - \mathbf{u}(\mathbf{p}_i))^2 + \sum_{i=1}^{n_\theta} \sum_{j=1}^{d-1} \left( (\mathbf{d}_i^T \nabla) \mathbf{u}^T(\mathbf{p}_{\theta_i}) \mathbf{e}_{i,j}^\perp \right)^2 \right) + \lambda J_m^d(\mathbf{u}), \quad (2)$$

where  $n$  is the number of pairs of point landmarks  $(\mathbf{p}_i, \mathbf{q}_i)$ .  $n_\theta$  is the number of orientations  $\mathbf{d}_i$  at locations  $\mathbf{p}_{\theta_i}$  in the source image. The vectors  $\mathbf{e}_{i,j}^\perp, j = 1 \dots d-1$  are perpendicular to the corresponding orientations  $\mathbf{e}_i$  at locations  $\mathbf{q}_{\theta_i}$  in the target image.  $J_m^d(\mathbf{u})$  is the smoothness-related energy term described in [4,5], where  $m$  is the order of derivatives used.  $L_i, i = 1 \dots n$  of (1) are bounded linear evaluation functionals. For the point constraints in the first sum of (2) we set  $L_i \mathbf{u} = \mathbf{u}(\mathbf{p}_i)$ , and for the orientation constraints in the double sum of (2) we set  $L_{i,j} \mathbf{u} = (\mathbf{d}_i^T \nabla) \mathbf{u}^T(\mathbf{p}_{\theta_i}) \mathbf{e}_{i,j}^\perp$ .  $\lambda$  is the regularization parameter. In case of  $\lambda = 0$ , we obtain an interpolation, and in the case of  $\lambda > 0$ , we obtain an approximation of the point and orientation constraints and a larger smoothness of the transformation. In the latter case, the orientation vectors should be normalized.

The second term in (2) is a scalar product between  $(\mathbf{d}_i^T \nabla) \mathbf{u}(\mathbf{p}_{\theta_i})$  and the vectors  $\mathbf{e}_{i,j}^\perp$ .  $(\mathbf{d}_i^T \nabla) \mathbf{u}(\mathbf{p}_{\theta_i})$  is the transformed orientation vector of the source image and it should be perpendicular to  $\mathbf{e}_{i,j}^\perp$ , the  $j$  orthogonal vectors of the orientation vector of the target image, such that its contribution to the functional is zero.

Choosing vectors from the orthogonal space has the advantage that the corresponding scalar product is zero independent of the length of the vectors. Note however, that this holds true only in the case of interpolation but not for approximation. The  $d-1$  perpendicular orientations  $\mathbf{e}_{i,j}^\perp$  to the target orientation vector  $\mathbf{e}_i$  constrain the orientation of the transformed source orientation vector  $\mathbf{d}_i$  to lie on a line. Accordingly, the number of constraints is lower if an orientation is not constrained w.r.t. a line, but w.r.t. a plane, for example. The landmark pairs  $(\mathbf{p}_{\theta_i}, \mathbf{q}_{\theta_i})$  with orientation information may, but need not be a subset of the landmark pairs  $(\mathbf{p}_i, \mathbf{q}_i)$ .

Application of the spline theorem in [5] yields the following solution to the minimizing functional in (2):

$$\begin{aligned}
\mathbf{u}(\mathbf{x}) &= \sum_{k=1}^M \sum_{j=1}^d a_{k,j} \phi_k(\mathbf{x}) \boldsymbol{\varepsilon}_j \\
&+ \sum_{i=1}^n \sum_{j=1}^d w_{1,i,j} U(\mathbf{x} - \mathbf{p}_i) \boldsymbol{\varepsilon}_j \\
&- \sum_{i=1}^{n_\theta} \sum_{j=1}^{d-1} w_{2,i,j} (\mathbf{d}_i^T \nabla) U(\mathbf{x} - \mathbf{p}_{\theta_i}) \mathbf{e}_{i,j}^\perp,
\end{aligned} \tag{3}$$

where  $\phi_1, \dots, \phi_M$  are the basis functions of the corresponding null-space of dimension  $M$ , and  $U(\mathbf{x})$  are radial basis functions depending on the used function space. Note, that in order to obtain bounded functionals  $L_i$  the used function space has to be constrained. As a consequence, we obtain for both cases of 2D and 3D registration incorporating orientations the function  $U(\mathbf{x}) = |\mathbf{x}|^3$  in (3) as the only possible solution for  $m = 2$ . The parameters  $\mathbf{a} = (a_{1,1}, a_{1,2}, \dots, a_{1,d}, a_{2,1}, \dots, a_{M,d})$  and  $\mathbf{w} = (w_{1,1,1}, \dots, w_{1,n,d}, \dots, w_{2,1,1}, \dots, w_{2,n_\theta,d-1})$  can be computed as the solution of the following system of linear equations:

$$\begin{aligned}
\mathbf{K}\mathbf{w} + \mathbf{P}\mathbf{a} &= \mathbf{v} \\
\mathbf{P}^T \mathbf{w} &= 0,
\end{aligned} \tag{4}$$

where  $\mathbf{K}$  and  $\mathbf{P}$  are matrices consisting of elements of the functions  $U(\mathbf{x})$ ,  $(\mathbf{d}_i^T \nabla)U(\mathbf{x})$ ,  $(\mathbf{d}_i^T \nabla)(\mathbf{d}_j^T \nabla)U(\mathbf{x})$ ,  $\phi(\mathbf{x})$ , and  $(\mathbf{d}_i^T \nabla)\phi(\mathbf{x})$ , respectively.  $\mathbf{v}$  is a vector corresponding to the target landmarks as well as zero values due to the scalar product of the orientations.

### 3 Experimental Results

Experiments with 2D and 3D synthetic as well as 2D tomographic data sets have been carried out. In medical images it is often important to distinguish between rigid and elastic parts of the image, e.g. rigid parts may be bones while the elastic parts correspond to soft tissue. With our synthetic experiments we have studied whether rigid parts can be mapped onto each other, while the elastic parts deform smoothly inbetween.

In Fig. 1 a translation of 60 pixels in each direction (first and second image) as well as a rotation of  $60^\circ$  around a spatially diagonal axis (third and fourth image) of a cube are shown (image size  $301 \times 301$  pixels), simulating both shape-preserving object shifts and rotations of objects in medical images, respectively. The edges of the cubes of the source images are drawn as outlines and each of the four images shows the transformed source image. Eight image border landmarks in the corners of the 3D images have been used to tie the whole image to its corners and another eight object landmarks have been used at the corners of the cube (see also the caption of Fig. 1).

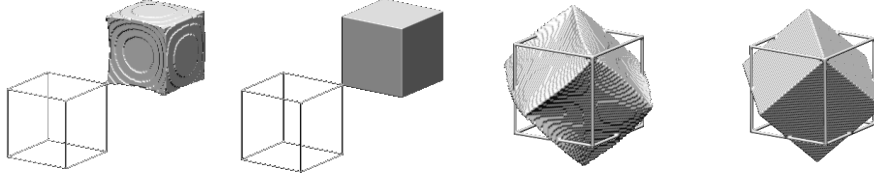


**Fig. 1.** Synthetic 3D data sets. Registration result of a translated (first and second image) and rotated (third and fourth image) cube. Thin-plate spline registration i) using only landmarks at each corner of the cube (object landmarks) and at each corner of the image (image border landmarks) (first and third image) as well as ii) with three orientations added to each object landmark (second and fourth image).

In case of translation (first and second image) we see that without orientation attributes (first image) the surfaces of the elastically transformed rigid cube become bended. In contrast, using orientation attributes at the cube's corners (second image), the surfaces of the rigid cube remain plane. Thus rigidity of the cube is preserved under translations. In case of rotation (third image) the surfaces and the edges of the cube become undulating. Using orientation attributes added at the corners of the cube, the cube's overall shape is much better preserved (fourth image).

In Fig. 2 an example of rotated rigid structures is shown (image size is  $181 \times 451$  pixels). The five rigid structures simulate a human spine (according to Little et al. [2]). In the second row of the figure the registration results are represented. We see that registration with landmarks only does not preserve the rigidity of the squares. When using orientation attributes and setting  $\lambda = 0$  (interpolation), we get a better registration result. The waviness of the outlines of the squares is reduced. In the last image of the figure we have used the approximation scheme with  $\lambda = 100$  and the same orientations as before. In this case we yield the best registration result. The structure of the squares is nearly preserved and the mean distance between the transformed source landmarks and the target landmarks is 0.5 pixels (the maximum is 1.3 pixels).

Fig. 3 gives an example for real image data. The first row shows two sagittal slices of two MR images of the brain of two different patients (on the left side is the source and on the right side the target image). We manually specified a number of 13 landmarks. In the second row on the left the registration result using landmarks only is shown. The white outlines of the target image are overlaid on the transformed source image. Improvement of this result can be achieved if we add further landmarks. However, specifying additional landmarks is often not possible. Therefore, we investigate the incorporation of orientation attributes at landmarks. In the second row on the right we have added one orientation at each of the landmarks No. 1 and 13. As a result we can see that the region between landmarks No. 1 and 2 (at the corpus callosum) is better registered than using landmarks only. However, the incorporation of orientations has also strong global effects, e.g., the region above the corpus callosum is deformed upwards.

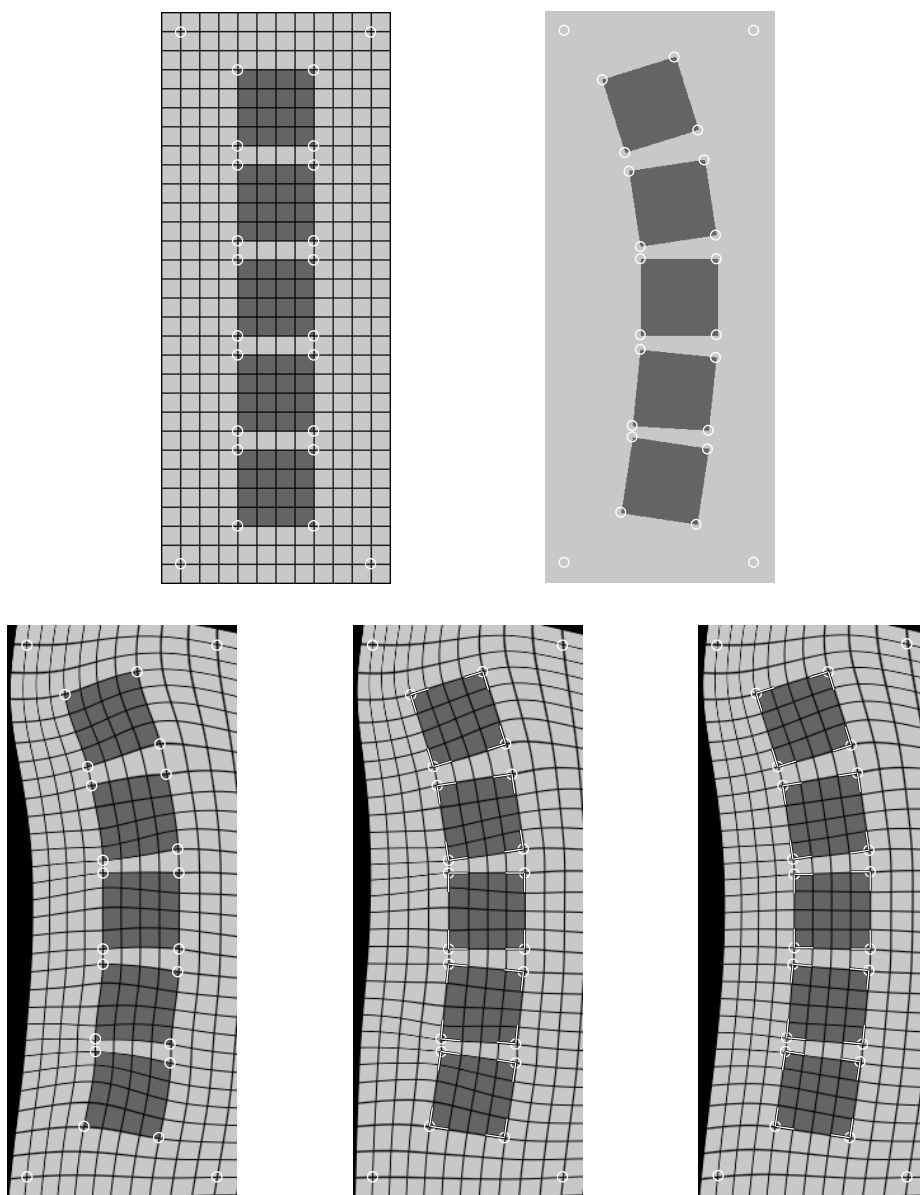


**Fig. 2.** Synthetic data set. Simulating a spine which is bended. First row: Source and target images. Second row: Registration using thin-plate splines with landmarks only (first), adding two orientations to each object landmark No. 5 to 24 (second), and using the approximation scheme with  $\lambda = 100$  and the same orientations as before (third).

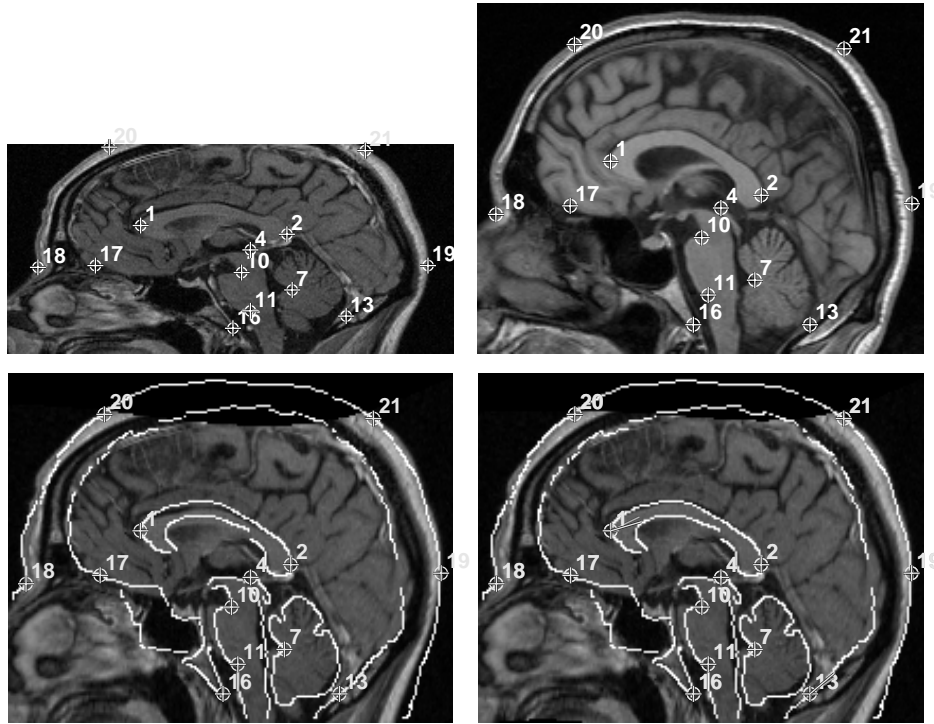


**Fig. 3.** Tomographic data sets. Two MR images of different brains with 13 landmarks, source and target images (first row). Second row: thin-plate spline registration using point landmarks only (left) and thin-plate spline registration using orientations at landmarks No. 1 and 13 (right).

## 4 Summary and Conclusion

We have demonstrated that by incorporating orientations in our elastic registration scheme it is possible to improve the registration accuracy without further adding landmarks. For synthetic images we have demonstrated that rigid structures can be preserved in an otherwise elastically deformed image. Experiments for tomographic data sets have shown that improvements can be obtained, but landmarks should be well-distributed in order to achieve good registration results. Future work will concentrate on how to limit the influence of the orientation constraints.

## Acknowledgement

This work has been supported by Philips Research Hamburg, project IMAGINE (Image- and Atlas-Guided Interventions in Neurosurgery).

## References

1. F. L. Bookstein and W. D. K. Green, “A Feature Space for Edgels in Images with Landmarks”, *Journal of Mathematical Imaging and Vision*, **3**, pp. 231–261, 1993
2. J. A. Little, D. L. G. Hill, and D. J. Hawkes, “Deformations Incorporating Rigid Structures”, *Computer Vision and Image Understanding*, **66**(2), pp. 223–232, 1997
3. K. V. Mardia, J. T. Kent, C. R. Goodall, and J. A. Little, “Kriging and splines with derivative information”, *Biometrika*, **83**(1), pp. 207–221, 1996
4. K. Rohr, H. S. Stiehl, R. Sprengel, W. Beil, T. M. Buzug, J. Weese, and M. H. Kuhn, “Point-Based Elastic Registration of Medical Image Data Using Approximating Thin-Plate Splines”, *Visualization in Biomedical Computing (VBC’96)*, Lecture Notes in Computer Science (1131), pp. 297–306, Springer, 1996
5. G. Wahba, “Spline Models for Observational Data”, *Society for Industrial and Applied Mathematics*, Philadelphia, Pennsylvania, USA, 1990